ACS OMEGA

http://pubs.acs.org/journal/acsodf

Article

Triazine-Based Functionalized Activated Carbon Prepared from Water Hyacinth for the Removal of Hg^{2+}, Pb^{2+}, and Cd^{2+} Ions from Water

Ahmad M. El-Wakil, Saadia M. Waly, Weam M. Abou El-Maaty, Mohamed M. Waly, Murat Yılmaz, and Fathi S. Awad*

Cite This: *ACS Omega* 2022, 7, 6058−6069

Read Online

ACCESS | Metrics & More | Article Recommendations | Supporting Information

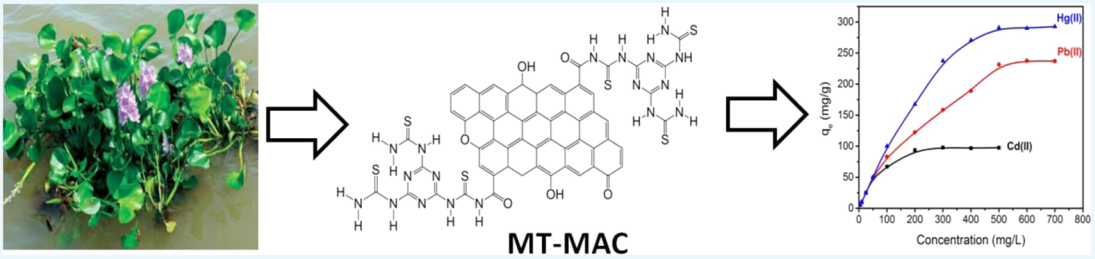

ABSTRACT: A novel chelating adsorbent, based on the functionalization of activated carbon (AC) derived from water hyacinth (WH) with melamine thiourea (MT) to form melamine thiourea-modified activated carbon (MT-MAC), is used for the effective removal of Hg^{2+}, Pb^{2+}, and Cd^{2+} from aqueous solution. Fourier transform infrared spectroscopy (FTIR), X-ray photoelectron spectroscopy (XPS), scanning electron microscopy (SEM), and Brunauer−Emmett−Teller (BET) theory confirm the successful functionalization of AC with the melamine thiourea chelating ligand through the amidation reaction between the carboxyl groups of oxidized activated carbon (OAC) and the amino groups of melamine thiourea (MT) in the presence of dicyclohexylcarbodiimide (DCC) as a coupling agent. The prepared MT-MAC exhibited extensive potential for the adsorption of the toxic metal ions Hg^{2+}, Pb^{2+}, and Cd^{2+} from wastewater. The MT-MAC showed high capacities for the adsorption of Hg^{2+} (292.6 mg·g^{-1}), Pb^{2+} (237.4 mg·g^{-1}), and Cd^{2+} (97.9 mg·g^{-1}) from aqueous solution. Additionally, 100% removal efficiency of Hg^{2+} at pH 5.5 was observed at very low initial concentrations (25−1000 ppb).The experimental sorption data could be fitted well with the Langmuir isotherm model, suggesting a monolayer adsorption behavior. The kinetic data of the chemisorption mechanism realized by the melamine thiourea groups grafted onto the activated carbon surface have a perfect match with the pseudo-second-order (PSO) kinetic model. In a mixed solution of metal ions containing 50 ppm of each ion, MT-MAC showed a removal of 97.0% Hg^{2+}, 68% Pb^{2+}, 45.0% Cd^{2+}, 17.0% Cu^{2+}, 7.0% Ni^{2+}, and 5.0% Zn^{2+}. Consequently, MT-MAC has exceptional selectivity for Hg^{2+} ions from the mixed metal ion solutions. The MT-MAC adsorbent showed high stability even after three adsorption−desorption cycles. According to the results obtained, the use of the MT-MAC adsorbent for the adsorption of Pb^{2+}, Hg^{2+}, and Cd^{2+} metal ions from polluted water is promising.

1. INTRODUCTION

After the industrial revolution, the industrial wastes from sewage sludge, textile printing, mining, fertilizers, pigments, electroplating, alkaline batteries, mining, textile printing, sewage sludge, and metallurgy are considered the primary sources of heavy metals (such as Hg^{2+}, Pb^{2+}, and Cd^{2+} ions) in water bodies. Heavy metals are highly toxic at very low concentrations.[1−4] Heavy metals accumulating in the human body can cause different chronic and severe diseases as anemia, hemoptysis, skeletal malformation, renal damage, impairment of pulmonary functions, emphysema, cancer, lung damage, nervous system damage, and hypertension.[5,6] As a result, various methods have been used for the removal of heavy metals from wastewaters such as electrodeposition,[7] bioremediation,[8−10] membrane separation,[11] flotation,[12] coagulation,[13] electrocoagulation,[14] ozonation,[15] and adsorption.[10,16,17]

Among these methods, adsorption using chelating resins is considered one of the most efficient methods for water treatment owing to its low cost, flexibility in operation, and design compared to those of other methods.[18−23] Many different materials have been used as adsorbents for the uptake of toxic substances from polluted water such as metal

Received: November 15, 2021
Accepted: February 3, 2022
Published: February 11, 2022

https://doi.org/10.1021/acsomega.1c06441
ACS Omega 2022, 7, 6058−6069

Scheme 1. General Process for the Synthesis of the Melamine Thiourea Ligand

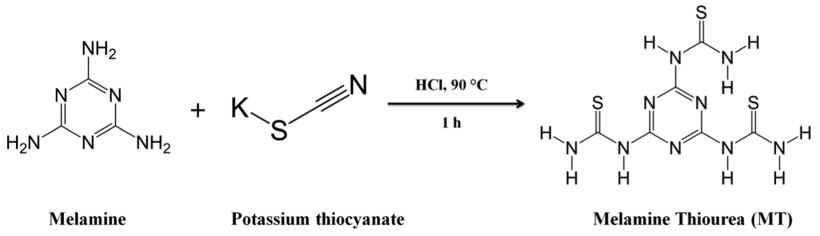

Scheme 2. General Process for the Synthesis of Melamine Thiourea-Chemically Modified Activated Carbon (MT-AMC)

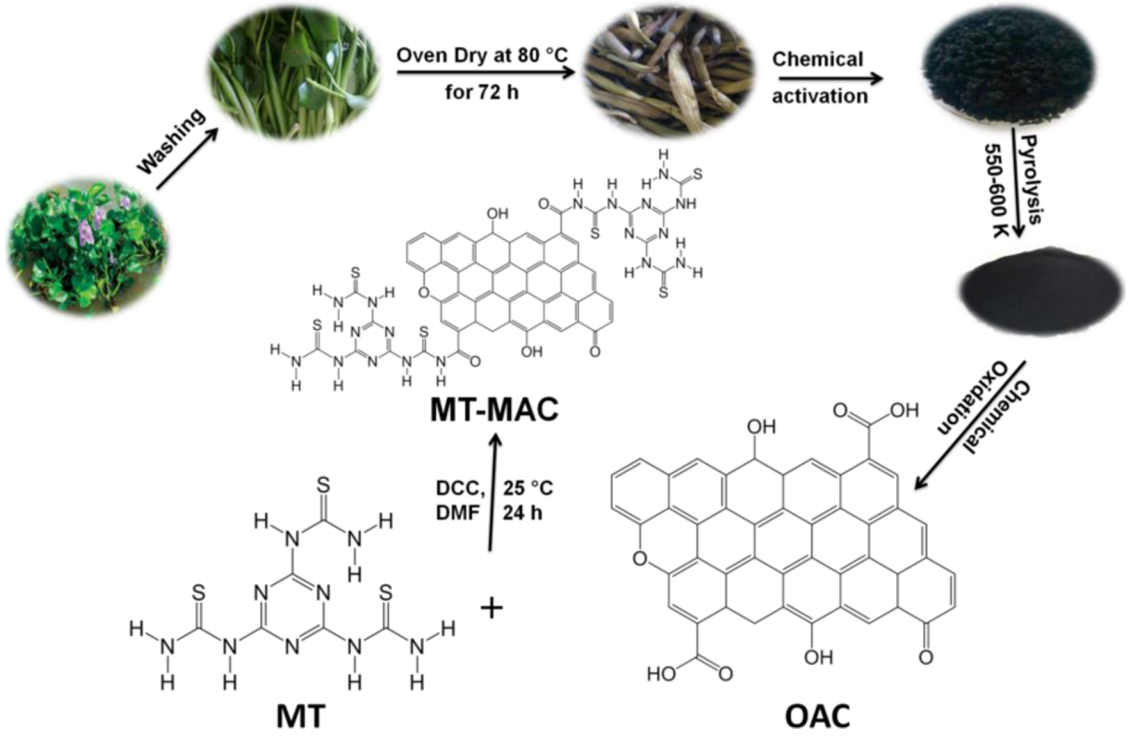

oxides,[24,25] activated carbon (AC),[26] covalent organic frameworks (COFs),[4,27] metal organic frameworks (MOFs),[28,29] minerals (clay),[30] inorganic nanomaterials,[31] agriculture wastes,[8,32] graphene oxide (GO),[33,34] and polymers.[35,36] Most of these adsorbents have low selectivity and capacity. Therefore, it is important to remove toxic metals from contaminated water using cheap and efficient adsorbents.

The most widely used adsorbent in lead removal is activated carbon due to its porous structure, high adsorption capacity, and high surface area. To improve the selectivity and capacity of activated carbon, several surface treatments with organic chelating agents have been applied to increase the number of functional groups. Various adsorbents have been developed such as sulfhydryl-functionalized activated carbon, 2-aminothiazole-functionalized activated carbon derived from water hyacinth,[16] and tris(hydroxymethyl)aminomethane-modified activated carbon.[5,6] The key challenge here is to functionalize activated carbon with active chelating ligands that can be used to extract cadmium ions from wastewater such as melamine derivatives.[37] Melamine is considered a strong chelating ligand because it has three free amine groups and three basic nitrogen atoms in the triazine ring with high binding ability toward heavy metals. Moreover, the amine groups on melamine can be used as an intermediate to introduce different functional groups to chelate heavy metals. Therefore, introducing ligands containing donor atoms such as sulfur will increase melamine's capacity toward heavy metals since its electron cloud can be easily polarized because it has a large size and nearly full d-electrons. For example, melamine was functionalized with thiourea, and then, it was used to extract Cd^{2+} from wastewaters.[37]

Herein, we introduce the novel adsorbent melamine thiourea for the effective removal of Hg^{2+}, Pb^{2+}, and Cd^{+2} ions from water with a remarkably high selectivity for Hg^{2+}. This particular modification for AC has never been reported before. The design strategy of MT-MAC was motivated by the introduction of amine and thiol groups onto the AC surface owing to their high binding ability to coordinate with mecury ions and form stable complexes. The general steps for the synthesis of MT-MAC are shown in Scheme 2. The method includes the oxidation of activated carbon derived from water hyacinth using nitric acid to increase the number of carboxylic acid groups on the AC surface followed by the amidation reaction between the carboxyl groups of oxidized activated carbon (OAC) and NH_2 groups of melamine thiourea (MT). The prepared MT-MAC adsorbent was characterized using Fourier transform infrared spectroscopy (FT-IR), Brunauer–Emmett–Teller (BET) theory, X-ray photoelectron spectroscopy (XPS), and scanning electron microscopy (SEM). The adsorption behavior of the prepared MT-MAC adsorbent

https://doi.org/10.1021/acsomega.1c06441
ACS Omega 2022, 7, 6058−6069

toward Hg^{2+}, Pb^{2+}, and Cd^{2+} was investigated using a batch process. The impacts of metal ion concentration, solution pH, temperature, and agitation time were evaluated. The kinetic, thermodynamic, and isotherm data were also studied.

2. EXPERIMENTAL SECTION

2.1. Synthesis of the Melamine Thiourea (MT) Active Ligand. The melamine thiourea active ligand preparation procedure is described below. In brief, 12 g of potassium thiocyanate (KSCN, Sigma-Aldrich, 99.0%) was dissolved in 100 mL of HCl (0.01 M) and 5 g of melamine (Sigma-Aldrich, 99.0%) was dissolved in 100 mL of pure water. After that, the KSCN solution was added to the melamine solution drop by drop with continuous stirring and then refluxed at 90°C. After 1 h, the bottle containing the solution was placed in an ice bath to cool; then, the sample was first centrifuged and then recrystallized with an ethanol−water mixture (1:1).[37] Scheme 1 shows the preparation procedure of the melamine thiourea (MT) active ligand.

2.2. Preparation of Melamine Thiourea-Chemically Modified Activated Carbon (MT-MAC). In this study, the water hyacinth (WH) plant, which is widely found and collected around the Nile River in Mansoura, Egypt, was used. After washing the dried water hyacinth (WH) first with faucet water and then with pure water, it was soaked in 0.25 M ethylenediaminetetraacetic acid (Sigma-Aldrich, 99.0%) (at pH 10) for 24 h to degrade the Hg^{2+}, Pb^{2+}, and Cd^{2+} ions present on the plant tissues. Then, it was washed a few times with pure water and left to dry in a furnace at 80 °C for 3 days. The first step in the preparation of AC was carried out by soaking dried water hyacinth in (50.0% v/v) H_3PO_4 solution (the solid mass to the acid solution volume was (1:3)) at room temperature (25 °C) for 48 h. Activation of the mixture, which was dehumidified for 2 days in an oven at 110 °C, was continued for 3 h at 550−600 K increasingly in an airless environment using a stainless-steel reactor. After the sample cooled down to room temperature, it was washed several times with distilled water until the acid in the filtrate was removed and left to dry in an oven at 120 °C. Increasing the number of functional groups such as aldehydes, hydroxyl, ketones, and carboxyl on the activated carbon surface by treating 3.0 g of activated carbon with 30 mL of HNO_3 (1:1) and refluxing for 3 h at 110 °C was aimed. The filtered adsorbent (OAC) was washed with pure water until the filtrate pH was stable at 6.0 and placed in a 120 °C oven to dry. MT-MAC was produced as follows: To a suspension of 500 mg of OAC adsorbent in anhydrous *N*,*N*-dimethyl formamide (DMF) (Sigma-Aldrich, 99.0%) (100 mL), 0.5 g of melamine thiourea (MT) and 1.0 g of *N*,*N*′-dicyclohexylcarbodiimide (DCC) (Sigma-Aldrich, 99.0%) were added, and the mixture was mixed at 25 °C for 1 day. The sample collected using filter paper in the last step was washed first with DMF and then with pure water and left to dry in a furnace at 80 °C for 1 day. Scheme 2 shows the preparation procedure of melamine thiourea-chemically modified activated carbon (MT-MAC).

2.3. Characterization. AC, OAC, and MT-MAC were characterized using Fourier transform infrared spectroscopy performed using a Jasco instrument (Model 6100, Japan) at a scanning range of 4000−400 cm^{-1}. XPS was carried out on a PHI Versa Probe III scanning XPS microprobe using ∼1.4 keV monochromatic Al Kα X-ray. BET surface areas of MT-MAC and OA were evaluated at 77 K using N_2 adsorption−desorption isotherms. Inductively coupled plasma optical emission spectroscopy (ICP-OES) with Ar^+ ion plasma gas equipped with a charged coupled detector (CCD) was used to determine the metal ion concentration.

2.4. Adsorption Equilibrium Studies. Using a shaking thermostat unit, we conducted batch adsorption experiments on Hg(II), Pb(II), and Cd(II) by shaking 10 mg of adsorbent in a 10 mL glass vial at different pH values (between 2.0 and 6.0), initial concentrations (between 10 and 800 ppm), temperatures (between 25 and 50 °C), and adsorbent doses (between 5 and 30 mg) at a constant shaking rate of 250 rpm. After each adsorption experiment, the adsorbents were removed from the solution, and the residual concentration of the metal ion was acidified with 2.0% HNO_3, and concentration measurements were carried out using inductively coupled plasma optical emission spectroscopy (ICP-OES) with Ar^+ ion plasma gas equipped with a charge-coupled detector (CCD). The amount of metal ions (q_e) adsorbed and the percentage % E can be calculated by eqs 1 and 2, respectively.

$$q_e = \frac{(C_0 - C_e)V}{m} \tag{1}$$

$$\%E = \frac{(C_0 - C_e)}{C_0} \times 100 \tag{2}$$

where C_0 and C_e are the initial and equilibrium heavy metal ion concentrations ($mg{\cdot}L^{-1}$), respectively, V (L) is the heavy metal ion solution volume, and m (g) is the weight of the samples.

2.4.1. Determination of pH_{PZC}. Solutions with pH between 2 and 12 were obtained by adding NaOH (0.1 M) or HCl (0.1 M) to Erlenmeyer flasks containing 50 mL of 0.01 M NaCl solution. Then, 0.15 g of the adsorbent was added to each flask; final pH measurements of the bottles were made after shaking for 48 h. The pH_{PZC} of the sample is calculated from the point where $pH_{final} = pH_{initial}$ crosses the curve between pH_{final} and $pH_{initial}$.

2.4.2. Adsorption Kinetic Studies. The adsorption kinetics of Pb^{2+}, Hg^{2+}, and Cd^{2+} onto MT-MAC were measured at equilibrium concentration and optimum pH. The solution was stirred continuously at 250 rpm at room temperatures, and samples were taken at different time intervals by rapid filtration from the solution. ICP-OES was used to determine the concentration of the Pb^{2+}, Hg^{2+}, and Cd^{2+} ions in the residual solution. Equilibrium adsorption capacities of adsorbents at time t, q_t (mg/g), are calculated using eq 1.

2.4.3. Desorption and Regeneration Studies. Desorption experiments were performed to evaluate the recovery of metal ions from the MT-MAC using HNO_3. For this purpose, 0.04 g of metal ion-loaded MT-MAC and 40 mL of of different eluents (0.1−0.5 M HNO_3, 0.5−3.0% thiourea) were mixed in a conical flask for 3 h. After this step, the adsorbents were separated by filtration, washed with pure water, and then neutralized with 0.1 M NaOH. The adsorbents regenerated by this method were used again for subsequent adsorption experiments.

3. RESULTS AND DISCUSSION

3.1. Characterization of AC, OAC, and MT-MAC. Scheme 2 shows the process of obtaining AC from water hyacinth (WH) with melamine thiourea (MT). The modification steps are listed below. In the first step, the melamine thiourea active ligand was prepared by the acid-catalyzed reaction between triazine triamine and potassium

https://doi.org/10.1021/acsomega.1c06441
ACS Omega 2022, 7, 6058−6069

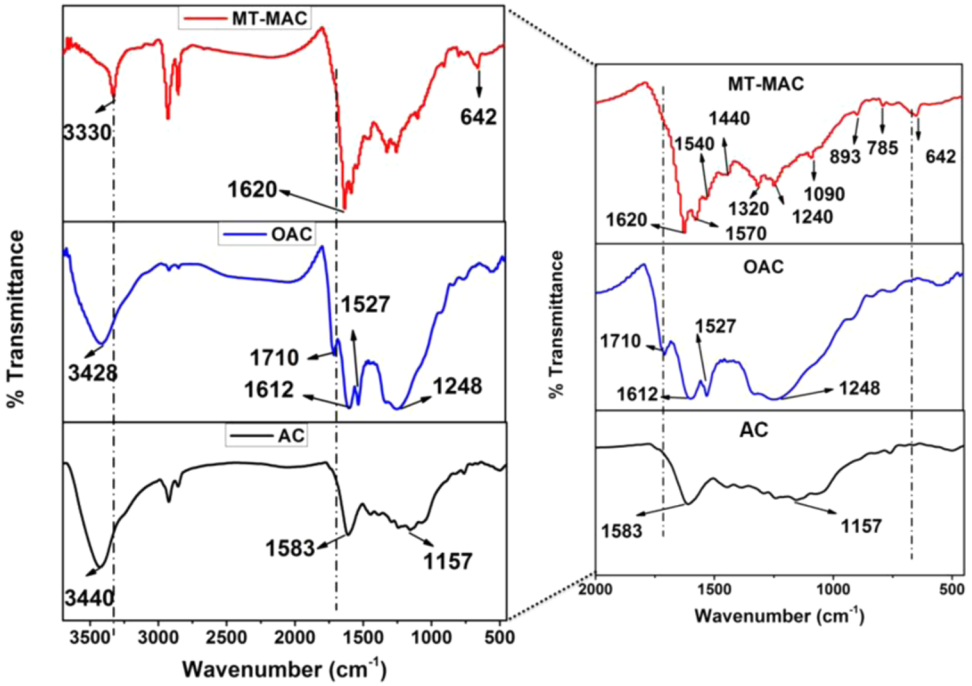

Figure 1. FTIR spectra of melamine thiourea-modified activated carbon.

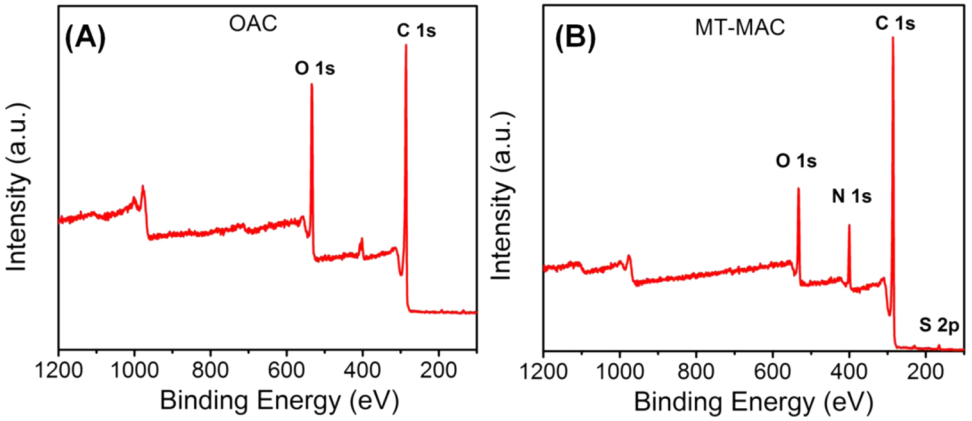

Figure 2. XPS survey spectra of OAC (A) and MT-MAC (B).

thiocyanate. In the second step, activated carbon was prepared from WH and then processed by chemical oxidation with nitric acid (HNO_3) to increase the number of carboxylic acid functional groups on the AC surface. In the third step, peptide bonds were formed due to the amidation reaction between the free NH_2 groups of melamine thiourea and the carboxylic acid groups of AC in the presence of *N*,*N*-dicyclohexylcarbodiimide (DCC) as a coupling agent.

To confirm the formation of the melamine thiourea active ligand from KSCN and melamine, Fourier transform infrared spectra were collected and are displayed in Figure S1. The FTIR spectrum of melamine exhibits peaks corresponding to the N−H stretching and bending oscillations in the region 3000−3500 and 1640 cm^{-1}, respectively. The peaks at 1021 and 578 cm^{-1} are ascribed to the triazine ring oscillations.[38,39] Additionally, the peaks between 1433−1533 and 810 cm^{-1} can be attributed to the stretching and bending oscillations of C−N. The FTIR spectrum of KSCN displays two distinguished peaks at 1641 and 2046 cm^{-1} corresponding to the bending and stretching oscillations of C═S, respectively.[40] Comparing the spectrum of melamine thiourea with that of melamine and KSCN, two new peaks at 655 and 1173 cm^{-1} corresponding to C−S bending and stretching oscillations are observed in the melamine thiourea spectrum, respectively.[37] These new peaks confirmed the formation of the melamine thiourea chelating ligand.[37]

The FTIR spectrum of AC is illustrated in Figure 1. The peaks at wavenumbers 3440, 2849−2932, and 1583 cm^{-1} are associated with aliphatic (CH), hydroxyl (OH), C═C (in the aromatic ring), and aromatic (C═C) stretching oscillations.[41] In addition, broad peaks, which are thought to belong to the C−O stretching oscillations in ethers, esters, and phenols, are observed in the wavenumber range of 1000−1300 cm^{-1}.[6,42] The changes observed as a result of the oxidation of activated carbon with nitric acid are illustrated in Figure 1 in the spectrum of AC. The two new peaks at 1612 and 1710 cm^{-1} correspond to the C═O stretching oscillations of ketones, lactones, aldehydes, and carboxylic groups.[6] As a result, the number of carboxyl functional groups on the activated carbon

https://doi.org/10.1021/acsomega.1c06441
ACS Omega 2022, 7, 6058−6069

surface increased as a result of the oxidation process with HNO_3.

Comparing the FTIR spectrum of OAC with that of MT-MAC, the C═O stretching oscillation of the COOH group in OAC disappeared, and new peaks are observed at 1620 and 1570 cm^{-1} that can be assigned to the C═O stretching oscillation of the NHCO (amide) and the bending oscillations of N−H in the NH_2 group, respectively.[2,43,44] Furthermore, the band at 3330 cm^{-1} in the MT-MAC spectrum can be assigned to the N−H stretching vibration of the secondary amine.[2,43,44] Also, new peaks are observed in the MT-MAC spectrum at 1240−1320, 1090, and 642 cm^{-1} assigned to C−N stretching oscillations (triazine), −C═S oscillations, and C−S oscillations, respectively.[2,6,43] The results obtained provide evidence of the successful functionalization of activated carbon with the melamine thiourea chelating ligand through amide linkage (peptide linkage).

The XPS plot shown in Figure 2 confirms the successful chemical modification of activated carbon from water hyacinth (WH) with the melamine thiourea (MT) chelating ligand. XPS was carried out on a PHI Versa Probe III scanning XPS microprobe using a ∼1.4 keV monochromatic Al Kα X-ray. When the XPS survey scans of OAC and MT-MAC were examined (Figure 2A,B respectively), the increase in the intensity of the C 1s peak also increased the intensity of the O 1s peak of MT-MAC. Additionally, two new peaks due to an S 2p and N 1s are observed in the MT-MAC survey scan.[2] These results indicate the successful covalent attachment of the melamine thiourea chelating ligand to the OAC surface through amide linkage (peptide linkage) where DCC is used as a binding agent.

The high-resolution C 1s spectrum (Figure S2A) attributed to the OAC was deconvoluted to four peaks with binding energies at 289.3 eV (C in COOH), 287.5 eV (C in C═O), 285.9 eV (C in C−O), and 284.9 eV (C in C−C, C═C).[2,45] Deconvolution of the C 1s spectrum of MT-MAC showed in Figure S2B identifies four peaks with binding energies at 288.6, 287.1, 286.3, and 284.6 eV corresponding to C−NH_2, C═N/N−C═O, C−O/C−S, and C−C/C═C, respectively.[2,44,46,47] Consequently, the chemical modification of OAC with MT was also evident from the peaks at 286.3, 287.2, and 288.6 eV for (C−S, C−N), (N−C═O, C═N), and C-NH_2, respectively. The high-resolution O 1s of OAC (Figure S2C) was deconvoluted to three peaks with binding energies at 531.5 eV (O in O−H), 532.5 eV (O in C═O), and 533.9 eV (O in COOH), while the O 1s spectrum of MT-MAC is deconvoluted to two peaks with binding energies at 531.2 eV (O in H−N−C═O) and 533.1 eV (O in C═O).[2,44,46,47] The successful incorporation of melamine thiourea onto the surface of OAC is also approved by the S 2p and N 1s spectra represented in Figure S2F,E, respectively. The high-resolution N 1s peak (Figure S2E) attributed to MT-MAC can be deconvoluted into two peaks with binding energies at 399.3 eV (N in C−N−C or C═N bonds) and 400.2 eV (N in N−C═O).[44] The high-resolution MT-MAC-related S 2p (Figure 2SF) dissociated into two peaks due to C═S and C-SOX bonds, with binding energies at 164.6 and 168.5 eV, respectively.[2,46] From FTIR and XPS analyses, the presence of C═N, O═C−N, C═S, C−S, and C−N peaks proves the successful functionalization of AC derived from WH with the melamine thiourea (MT) chelating ligand.

Surface areas of MT-MAC and OA were evaluated at 77 K using N_2 adsorption−desorption isotherms. The results are plotted in Figure 3, and they showed a typical type (I) isotherm for OAC, which is a characteristic for microporous

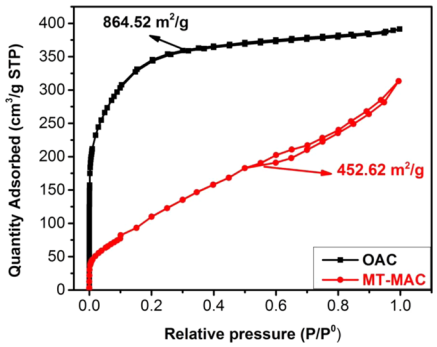

Figure 3. N_2 adsorption−desorption isotherms for OAC and MT-MAC.

materials, and a typical type (V) isotherm for MT-MAC with a hysteresis loop, which is a characteristic for mesoporous materials according to the IUPAC classification of porous materials. The surface area of OAC (864.52 m^2 g^{-1}) was much higher than that of MT-MAC (452.62 m^2 g^{-1}). Table S1 illustrates the BET surface areas of OAC and MT-MAC adsorbents.

The results showed that the pore volume of OAC (0.5216 cm^3/g) is much higher than the pore volume of MT-MAC (0.2916 cm^3/g). The high pore volume and surface area of OAC could be attributed to nitric acid treatment after the carbonization step, which can play an important role in cleaning the surface's impurities that block the pores on the surface and also generating new pores.[48] Additionally, the treatment with nitric acid leads to the formation of nitric dioxide and carbon dioxide gases that increase the porosity of OAC.[48] Therefore, these results prove the role of nitric acid treatment in generating a porous surface.

Comparing the surface area of OAC with that of MT-MAC, a sharp decrease in the pore volume, pore size, and specific surface area is observed. The pore volume and the specific surface area of MT-MAC were reduced to 0.2916 cm^3/g and 493.78 m^2/g, respectively. This may be attributed to the chemical modification with MT chelating ligands that would occupy a certain space in the AC pore, and binding to the surface of AC would block part of the pores. These results, consistent with FTIR, XPS, and SEM, confirm the successful functionalization of oxidized activated carbon by melamine thiourea chelating ligands.

OAC and MT-MAC morphologies were specified using a scanning electron microscopy (SEM) instrument (JSE-T20 (JEOL, Japan) model) and are displayed in Figure 4. Evenly distributed honeycomb or circular holes visible on the surface of OAC in Figure 4 indicate that the surface is smooth and porous. After chemical modification with melamine thiourea, OAC became coarser and crumpled with a more irregular pore structure.

3.2. pH Effect on Hg^{2+}, Pb^{2+}, and Cd^{2+} Adsorption. The dependence of Pb^{2+}, Hg^{2+}, and Cd^{2+} adsorption onto MT-MAC at the initial solution pH is shown in Figure 5A. It can be understood that when the solution pH increases from 2 to 6, the sorption capacity increases. It is observed that Pb^{2+}, Hg^{2+}, and Cd^{2+} removals are low at low pH values due to the competition between heavy metal ions and H^+ ions in the adsorption free sites of MT-MAC. The small size of the H^+ ion

https://doi.org/10.1021/acsomega.1c06441
ACS Omega 2022, 7, 6058−6069

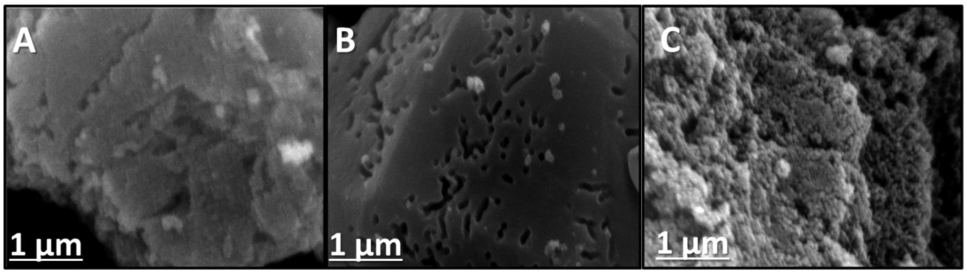

Figure 4. SEM images of (A) AC, (B) OAC, and (C) MT-MAC.

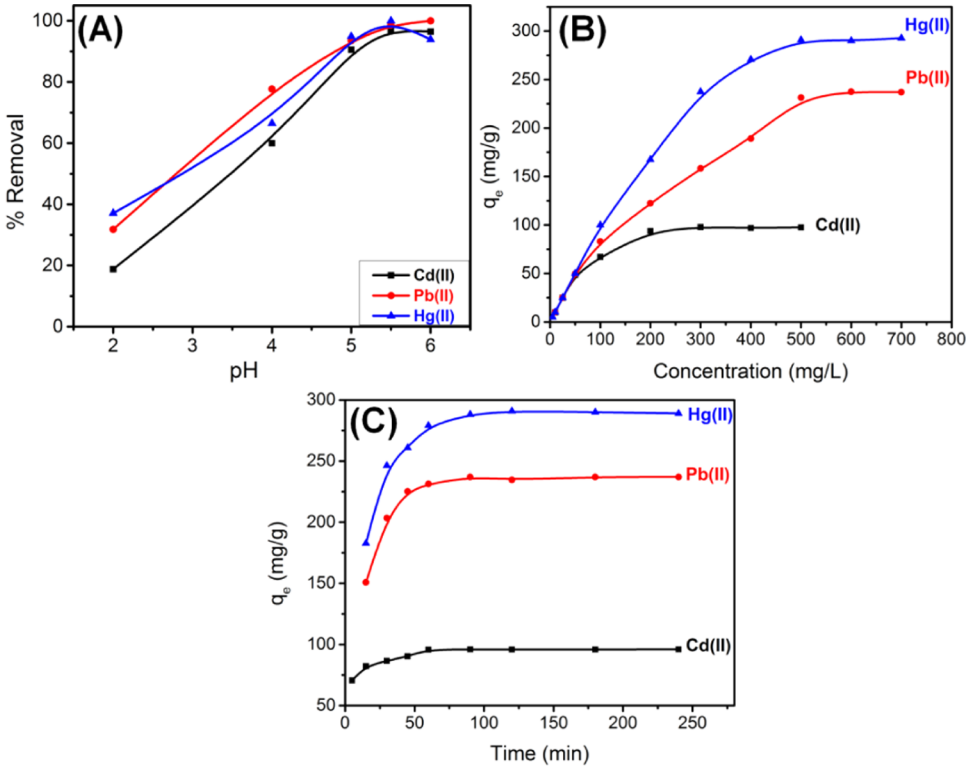

Figure 5. (A) Effect of solution pH on MT-MAC's adsorption of Pb^{2+}, Hg^{2+}, and Cd^{2+} ions (Pb^{2+} = 100 mg·L^{-1}, Hg^{2+} and Cd^{2+} = 50 mg·L^{-1}, adsorbent = 1.0 g·L^{-1}, and Temp. = 25 ± 2 °C). (B) Effect of the initial concentration on MT-MAC's adsorption of Pb^{2+}, Hg^{2+}, and Cd^{2+} ions (Pb^{2+} and Hg^{2+} = 10−700 mg·L^{-1}, Cd^{2+} = 10−500 mg·L^{-1}, adsorbent = 1.0 g·L^{-1}, pH = 5.5, and Temp. = 25 ± 2 °C). (C) Effect of contact time on MT-MAC's adsorption of Pb^{2+}, Hg^{2+}, and Cd^{2+} ions (Pb^{2+} and Hg^{2+} = 500 mg·L^{-1}, Cd^{2+} = 200 mg·L^{-1}, adsorbent = 1.0 g·L^{-1}, pH = 5.5, and Temp. = 25 ± 2 °C).

makes it a strong competitor for adsorption. Additionally, MT-MAC comprised surface functional groups such as amine, hydroxyl, amide, thiol, and carboxyl, which are influenced by the pH of the solution.[2,21−23] At low pH values, the surface functional groups of MT-MAC are protonated. However, with the increase of solution pH values from 2 to 5.5, the degradation efficiency of Pb^{2+}, Hg^{2+}, and Cd^{2+} increased from 24.45 to 100.0% (for Hg^{2+}), from 36.6 to 100.0% (for Pb^{2+}), and from 78.3 to 98.3% (for Cd^{2+}) because the −COOH, $-NH_2$, O═C−NH_2, and -OH are deprotonated and easy to bind with the Pb^{2+}, Hg^{2+}, and Cd^{2+} ions. If the effect of pH is to be examined in terms of pH_{pzc} of the adsorbent, the total surface charge is zero because the numbers of negative and positive groups in pH_{pzc} are equal. The pH_{pzc} values of the adsorbents AC, OAC, and MT-MAC were 4.05, 3.38, and 3.98, respectively. At lower pH, the activated carbon is positively charged (pH < pH_{PZC}), resulting in electrostatic repulsion between the heavy metal ions and the positively charged surface. Since the surface charge density decreases, with an increase in the solution pH (pH > pH_{PZC}), the adsorbent surface becomes negatively charged, leading to enhancement of electrostatic attraction between the carbon surface and the Pb^{2+}, Hg^{2+}, and Cd^{2+} ions. All adsorption experiments were conducted at pH 5.5 to avoid the precipitation of heavy metal ions as metal hydroxide $M(OH)_2$.

3.3. Adsorption Isotherms. The impact of Hg^{2+}, Pb^{2+}, and Cd^{2+} concentration on the extraction of Hg^{2+}, Pb^{2+}, and Cd^{2+} by melamine thiourea-modified activated carbon was studied at optimum pH = 5.5, and the results are graphed in Figure 5B. The results showed that the number of heavy metal ions removed onto MT-MAC increased with an increase in the concentration of heavy metal ions till equilibrium was reached. Due to the higher driving force of the concentration gradient, the adsorption capacity, mass transfer, and the availability of vacant binding sites (COOH, NH_2, O═C−NH_2, and SH) for metal ions are increased.[2,18,49,50] When the initial concentrations of Pb^{2+}, Hg^{2+}, and Cd^{2+} ions (10 ppm for all three) are increased to 800, 800, and 500 ppm, respectively. The amount

https://doi.org/10.1021/acsomega.1c06441
ACS Omega 2022, 7, 6058−6069

Table 1. Estimated Constants of Langmuir and Freundlich Isotherms for the Adsorption of Pb^{2+}, Hg^{2+}, and Cd^{2+} ions over MT-MAC

	Langmuir parameters					Freundlich parameters		
metal ion	R^2	b (L/mg)	$Q_{max,\ calc}$ (mg/g)	Q_{exp} (mg/g)	R_L	R^2	K_f	$1/n$
Hg^{2+}	0.997	14.782	310.559	292.60	0.0001	0.794	92.158	0.205
Pb^{2+}	0.964	5.109	259.740	237.44	0.0004	0.959	29.247	0.347
Cd^{2+}	0.999	22.09	98.520	97.90	0.0001	0.938	45.370	0.136

of metal ions adsorbed at equilibrium (q_e) changes from 10 to 292.6 mg/g for Hg^{2+}, It increased from 10 to 237.0 mg/g for Pb^{2+} and from 9.8 to 97.9 mg/g for Cd^{2+}. A 100.0% removal of Hg(II) at pH 5.5 was observed at low concentrations (25−1000 ppb), as shown in Figure S3.

Figures S5A and S4A show the Langmuir and Freundlich adsorption isotherm models obtained from the experimental data, respectively. Equation 3 shows the mathematical expression of the Langmuir isotherm model.[51,52]

$$\frac{C_e}{q_e} = \frac{1}{bQ} + \frac{C_e}{Q} \tag{3}$$

where C_e, q_e, b, and Q are the equilibrium concentration of the heavy metal ions, the equilibrium adsorption capacity, the Langmuir constant, and the Langmuir monolayer adsorption capacity, respectively.

The constant b is used in the calculation of the R_L value as shown in eq 4. Equation 4 can be used to predict whether the shape of the isotherm will be irreversible ($R_L = 0$), linear ($R_L = 1$), negative ($R_L > 1$), or positive ($0 < R_L < 1$).[51,52]

$$R_L = \frac{1}{1 + bC_0} \tag{4}$$

The linear form of the Freundlich isotherm model, which is based on the assumption multilayer adsorption occurring on heterogeneous surfaces, is as follows[44,45]

$$\ln q_e = \frac{1}{n}\ln c_e + \ln k_F \tag{5}$$

where k_F and $1/n$ represent the Freundlich constant and adsorption density, respectively, and can be calculated from the intercept and slope of the linear graph shown in Figure S4A. The parameters of both models were calculated and are summarized in Table 1. It can be understood from the results that the experimental data are compatible with the Langmuir adsorption isotherm model with high (R^2) values. In addition, the values calculated from the theoretical model equation showed excellent agreement with the experimental data. R_L values between 0 and 1 also indicate positive adsorption, as shown in Table 1.

3.4. Adsorption Kinetics. The effect of contact time on the removal of Hg^{2+}, Pb^{2+}, and Cd^{2+} ions on MT-MAC was evaluated between 10 and 240 min, keeping other parameters constant. The results are presented in Figures 5C and S4B. The contact time required to reach the maximum adsorption capacities was determined as 60 min for Cd^{2+} and Hg^{2+} and 90 min for Pb^{2+}. It is understood from the adsorption kinetics that 87.0, 93.0, and more than 85.0% of MT-MAC adsorption capacities occur in the first 15 min for Hg^{2+} and Cd^{2+} and in the first 30 min for Pb^{2+}, respectively. The fact that the adsorption is very fast at first is related to the abundance of void adsorption sites on the surface of the MT-MAC adsorbent, and the adsorption rate decreases over time as these gaps are filled.[18,19,44,45]

The pseudo-first-order (PFO) kinetic model and pseudo-second-order (PSO) kinetic model equations were used to explain the adsorption mechanism of Hg^{2+}, Pb^{2+}, and Cd^{2+} ions on the MT-MAC adsorbent. The PFO kinetic model and PSO kinetic model equations are given in eqs 6 and 7, respectively[34−45]

$$\log(q_e - q_t) = \log q_e - \frac{K_1 t}{2.303} \tag{6}$$

$$\frac{t}{q_t} = \frac{1}{K_2 q_e^{\ 2}} + \frac{t}{q_e} \tag{7}$$

where q_e and q_t represent Hg^{2+}, Pb^{2+}, and Cd^{2+} ions adsorbed at equilibrium and at time t (min), respectively, and k_1 (min^{-1}) and k_2 ($g{\cdot}mol^{-1}{\cdot}min^{-1}$) are rate constants. The t/q_t vs t plot should be linear; when k_1 values were calculated from the graphs between $\log(q_e - q_t)$ and t (Figure S4B), R^2 (correlation coefficient) and k_2 (rate constant) were calculated from the data (Figure S5B). Table S2 summarizes the calculated kinetic parameters.

Table S2 shows that the correlation coefficients (R^2) of the PSO kinetic model ($R^2 \ll 0.999$) are greater than those of the PFO kinetic model. In addition, the experimental values (qe_{exp}) show compatibility with the calculated maximum adsorption capacity (qe_{cal}). This showed that the adsorption of Hg^{2+}, Pb^{2+}, and Cd^{2+} ions on MT-MAC can be well-described using the PSO model, in which electron sharing or exchange occurs between MT-MAC adsorbents and metal ions.[21,47]

3.5. Effect of Temperature and Adsorbent Dosage. The effect of temperature on the adsorption capacities of Hg^{2+}, Pb^{2+}, and Cd^{2+} ions onto MT-MAC was studied at temperatures of 25 and 50 °C. The experimental data are depicted in Figure S6A. The maximum adsorption capacities of Hg^{2+}, Pb^{2+}, and Cd^{2+} ions increased from 290 to 332.7 mg/g, from 237.4 to 245.45 mg/g, and from 97.5 to 112.5 mg/g, respectively, with increasing temperature from 25 to 50 °C. The increase in the maximum adsorption capacity of heavy metal ions is probably related to the increase in the kinetic energy and mobility of the ions in a solution with a high temperature.[44]

The effect of adsorbent doses (5, 10, 15, 20, and 30 mg/10 mL) is shown in Figure S6B. It could be seen that when the amount of adsorbent dose increases from 5.0 to 30.0 mg, the percentage of removal of 500 ppm Hg^{2+}, 500 ppm Pb^{2+}, and 100 pm Cd^{2+} increases from 37.07 to 83.84%, from 30.80 to 88.72%, and from 50.90 to 99.60%, respectively. This situation allows the increase of the adsorbent dose to increase the total surface area, which allows the presence of more sorption sites.

3.6. Mechanism of Removal. To further analyze the mechanism of Cd^{2+} adsorption onto MT-MAC, the FTIR and XPS spectra of MT-MAC after Cd^{2+} adsorption were measured. It can be seen from Figure 6 that some bands

https://doi.org/10.1021/acsomega.1c06441
ACS Omega 2022, 7, 6058−6069

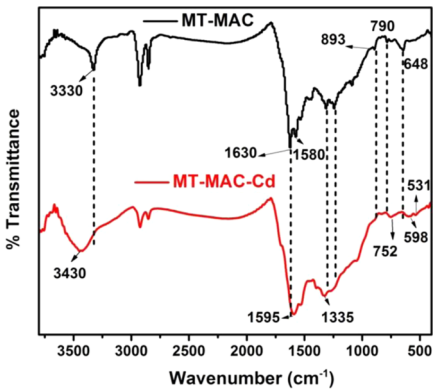

Figure 6. FTIR spectra of MT-MAC before and after Cd^{2+} adsorption.

shift to lower or higher wavenumbers, confirming that amine, amide, thiol, and hydroxyl groups play a role in Cd^{2+} adsorption. When the FTIR spectra of Cd^{2+} adsorption were examined, the change observed before and after adsorption was that the stretch vibration peak of secondary amines at 3330 cm^{-1} shifted to 3430 cm^{-1}; this peak became wider and less dense, and this situation showed adsorption of Cd^{2+} ions on amine groups. Additionally, the stretching vibration band at 1630 cm^{-1} (C═O in O═C−NH) and N−H stretching vibration at 1580 cm^{-1} are shifted to 1595 and 1524 cm^{-1}, respectively.[53−55] Also, the peaks of the MT-MAC spectrum at 790 and 648 cm^{-1} owing to −C═S vibrations and C−S vibrations, respectively, are shifted to 752 and 598 cm^{-1}. Moreover, a new peak at 531 cm^{-1} (Figure 6) was attributed to the stretching vibration of the S−Cd. This suggestion is also confirmed by the analysis of the XPS N 1s and S 2p spectra of MT-MAC after Cd^{2+} adsorption as shown in Figure 7A−D. After cadmium adsorption, the N 1s spectra showed fitted peaks centered around 402.1, 401.5, and 398.58 eV corresponding to Cd−N−C═O, Cd−N═C, and Cd−N−C, respectively. Additionally, the S 2p spectra after Cd adsorption exhibited peaks at 164.6, 164.1, and 163.8 and 162.8 eV due to Cd−S═C, C−S−Cd, and S−Cd, respectively. These observations confirm that the mechanism of removal of Cd^{2+} on the surface of MT-MAC involves surface complexation between the Cd^{2+} ions and amine, amide, thiol, and hydroxyl groups, as shown in Figure S7.

3.7. Desorption and Reusability Studies. An important parameter sought after in an effective adsorbent is the reusability of the adsorbent. The results of desorption studies of Pb^{2+}, Hg^{2+}, and Cd^{2+} heavy metal ions from the surface of MT-MAC revealed that 96.0, 99.0, and 100.0% desorption of Hg^{2+}, Pb^{2+}, and Cd^{2+} MT-MAC was accomplished using 0.5 M HNO_3, whereas 100% desorption of Hg^{2+}, Pb^{2+}, and Cd^{2+} was accomplished using (0.1 M HNO_3 + 4% thiourea). According to these results, it is possible to use MT-MAC a few times to adsorb and desorb Hg^{2+}, Pb^{2+}, and Cd^{2+} since the desorption reaches about 100.0% from the adsorbent surface. The reusability of the MT-MAC adsorbent was investigated by repeating the adsorption−desorption process three times by preparing solutions with a concentration of 100 ppm for Hg^{2+} and Pb^{2+} and 50 ppm for Cd^{2+} and using the same adsorbent each time. Figure 8 shows the recycling of the MT-MAC adsorbent for Hg^{2+}, Pb^{2+}, and Cd^{2+} ions. The results revealed that after three adsorption−desorption cycles, the adsorbent still has a removal efficiency higher than 92.0% (Hg^{2+}), 85.0%

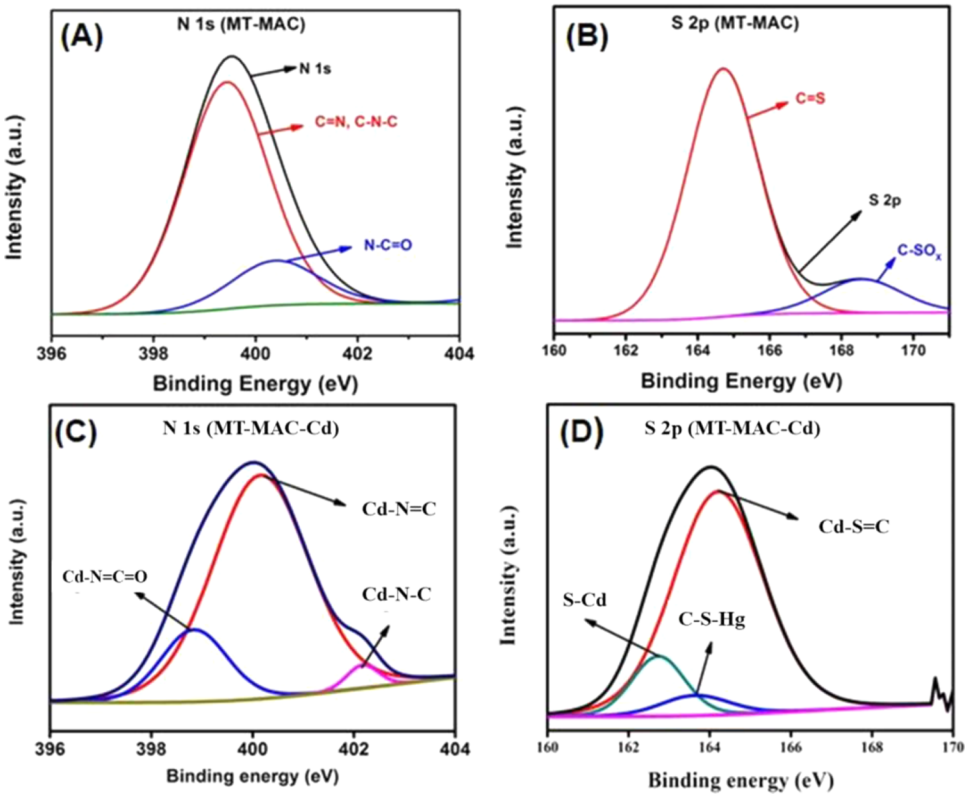

Figure 7. XPS high-resolution spectra of N 1s in MT-MAC before adsorption (A), N 1s in MT-MAC after Cd^{2+} adsorption (C), S 2p in MT-MAC before Cd^{2+} adsorption, (B) and S 2p in MT-MAC after Cd^{2+} adsorption (D).

https://doi.org/10.1021/acsomega.1c06441
ACS Omega 2022, 7, 6058−6069

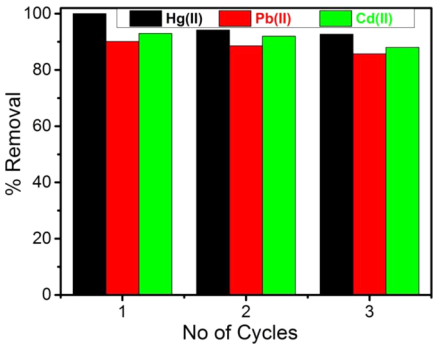

Figure 8. Reusability of MT-MAC adsorbents for Hg^{2+}, Pb^{2+}, and Cd^{2+} ($Hg^{2+}$and Pb^{2+} = 100 mg·L^{-1}, Cd^{2+} = 50 mg·L^{-1}, adsorbent = 1.0 g·L^{-1}, pH 5.5, and desorbing agent: 0.5 M HNO_3).

(Pb^{2+}), and 88.0% (Cd^{2+}). Consequently, MT-MAC is an effective and cheap adsorbent for the adsorption of Pb^{2+}, Hg^{2+}, and Cd^{2+} ions from wastewater.

3.8. Selectivity of MT-MAC for the Removal of Mercury Ions. The selectivity of MT-MAC for the removal of mercury ions was evaluated by adding 0.05 g of MT-MAC to a vial containing 5 mL of multiple-metal ion system (Hg^{2+}, Pb^{2+}, Cu^{2+}, Ni^{2+}, Cd^{2+}, and Zn^{2+}). The results revealed that the percentage of removal of Hg(II) is higher than that of other metal ions (Figure 9). Consequently, MT-MAC has exceptional selectivity for Hg(II) ions from the mixed metal ion solutions.

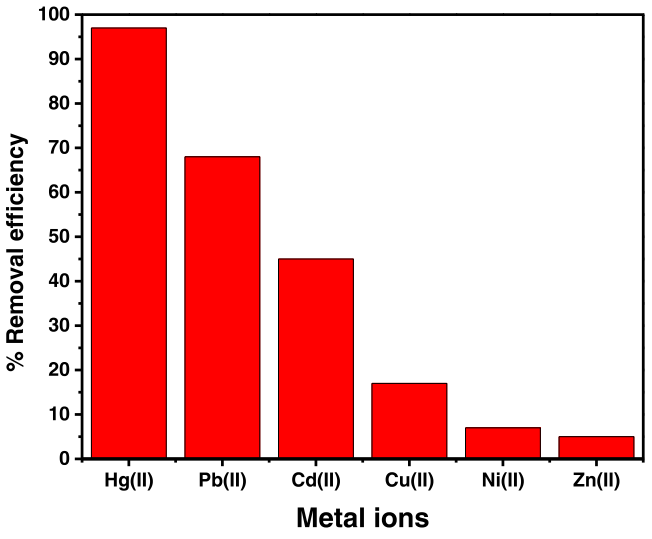

Figure 9. Metal ion removal on MT-MAC from a mixed solution of metal ions (C_0 = 50 mg/L, pH = 5.5, T = 298 K, and m/V = 1 g/L).

3.9. Comparison with Results Reported in the Literature. Table 2 compared the adsorption capability of the proposed MT-MAC sorbents in the adsorption of Pb^{2+}, Hg^{2+}, and Cd^{2+} heavy metal ions from water with that of some other work. These data clarify the strength of chemically modified activated carbon in the adsorption of Pb^{2+}, Hg^{2+}, and Cd^{2+} from aqueous solutions. The high adsorption capacity for MT-MAC could be attributed to the amine and thiol groups on the surface of AC with tremendous ability to chelate cadmium ions directly from the solution compared with other carbon-based materials.

Table 2. Comparison of Adsorption Capacity of the Proposed Adsorbents with Some Sorbents Reported for the Adsorption of Hg^{2+}, Pb^{2+}, and Cd^{2+}

heavy metals	adsorbents	$q_{e\ max}$ (mg·g^{-1})	ref
Hg^{2+}	MT-MAC	292.6	this work
	activated carbon functionalized with thiol groups	235.7	1
	graphene oxide functionalized with thiosemicarbazide	231.0	46
	nitrogen-doped carboxylated porous carbon	257.0	56
	polyacrylonitrile-modified partially reduced graphene oxide composites	324.0	45
	thiol- and amine-incorporated UIO-66-NH_2	580.0	17
Pb^{2+}	MT-MAC	237.4	this work
	activated carbon obtained from pistachio wood	190.2	57
	mangosteen peel activated carbon	130.0	58
	graphene oxide modified with 2,2′-dipyridylamine	369.75	33
	nitrogen-doped carboxylated porous carbon	721.0	56
	sulfhydryl-functionalized activated carbon	116.3	6
Cd^{2+}	MT-MAC	97.9	this work
	jackfruit leaf	20.3	10
	amine-functionalized activated carbon	79.2	21
	AC prepared from *Leucaena leucocephala* biomass	70.4	23
	silicon/aluminum nanomaterial	61.8	59
	magnetic carbon aerogel	143.8	60
	graphene oxide modified with 2,2′-dipyridylamine	257.2	33

4. CONCLUSIONS

We have developed a novel chelating adsorbent, MT-MAC, for Hg^{2+}, Pb^{2+}, and Cd^{2+} removal. The MT-MAC adsorbents exhibited a fast adsorption rate and high adsorption capacity for Hg^{2+}, Pb^{2+}, and Cd^{2+} at room temperature. Based on equilibrium isotherms and adsorption kinetics of Pb^{2+}, Hg^{2+}, and Cd^{2+} onto MT-MAC, the maximum adsorption capacities for Hg^{2+}, Pb^{2+}, and Cd^{2+} onto MT-MAC were 292.9, 237.4, and 97.9 mg/g, respectively, which were much higher than those reported previously. The rate of adsorption is rapid, with about 90% removal within 15 min, and the maximum adsorption capacities for Hg^{2+}, Pb^{2+}, and Cd^{2+} onto MT-MAC were 292.9, 237.4, and 97.9 mg/g, respectively. The Langmuir isotherm model and pseudo-second-order kinetic model were used successfully to discuss the isotherms of metal ion removal and adsorption kinetics, respectively. Based on FTIR, the chemisorption mechanism was proposed. Metal ions could be regenerated from the MT-MAC adsorbent using 0.5 M HNO_3 or (0.1 M HNO_3 + 4% thiourea). Additionally, MT-MAC showed high stability over three adsorption−desorption cycles. On the basis of the data of the present study, MT-MAC is an efficient and eco-friendly adsorbent for heavy metal removal from wastewater.

■ ASSOCIATED CONTENT

Supporting Information

The Supporting Information is available free of charge at https://pubs.acs.org/doi/10.1021/acsomega.1c06441.

https://doi.org/10.1021/acsomega.1c06441
ACS Omega 2022, 7, 6058−6069

FTIR spectra of melamine, KSCN, and melamine thiourea ligands, XPS high-resolution spectra of C 1s, N 1s, and S 2p in OAC and MT-MAC, dependence of the removal efficiency of Hg(II) on the initial concentration, linear form of the Freundlich isotherm and PFO of Hg^{2+}, Pb^{2+}, and Cd^{2+} adsorption over MT-MAC, linear form of yjr Langmuir isotherm and pseudo-second-order kinetic model for Hg(II), Pb(II), and Cd(II) adsorption onto MT-MAC, dependence of the adsorption of Hg^{2+}, Pb^{2+}, and Cd^{2+} ions onto MT-MAC on the adsorbent dosage and temperature, proposed mechanism for the removal of Cd^{2+} by strong interactions with nitrogen and sulfur atoms on the surface of MT-MAC, surface area and pore volume of OAC and MT-MAC, and kinetic parameters for the adsorption of Hg^{2+}, Pb^{2+}, and Cd^{2+} ions onto MT-MAC (PDF)

AUTHOR INFORMATION

Corresponding Author

Fathi S. Awad − *Chemistry Department, Faculty of Science, Mansoura University, Mansoura 35516, Egypt*; orcid.org/0000-0002-9907-0695; Email: fathyawad949@yahoo.com

Authors

Ahmad M. El-Wakil − *Chemistry Department, Faculty of Science, Mansoura University, Mansoura 35516, Egypt*

Saadia M. Waly − *Chemistry Department, Faculty of Science, Mansoura University, Mansoura 35516, Egypt*

Weam M. Abou El-Maaty − *Chemistry Department, Faculty of Science, Mansoura University, Mansoura 35516, Egypt*

Mohamed M. Waly − *Chemistry Department, Faculty of Science, Mansoura University, Mansoura 35516, Egypt*

Murat Yılmaz − *Department of Chemical Engineering, Faculty of Engineering, Osmaniye Korkut Ata University, 80000 Osmaniye, Turkey*

Complete contact information is available at: https://pubs.acs.org/10.1021/acsomega.1c06441

Notes

The authors declare no competing financial interest.

REFERENCES

(1) Xia, S.; Huang, Y.; Tang, J.; Wang, L. Preparation of various thiol-functionalized carbon-based materials for enhanced removal of mercury from aqueous solution. *Environ. Sci. Pollut. Res.* **2019**, *26*, 8709−8720.

(2) Awad, F. S.; AbouZeid, K. M.; El-Maaty, W. M. A.; El-Wakil, A. M.; El-Shall, M. S. Efficient removal of heavy metals from polluted water with high selectivity for mercury (II) by 2-imino-4-thiobiuret−partially reduced graphene oxide (IT-PRGO). *ACS Appl. Mater. Interfaces* **2017**, *9*, 34230−34242.

(3) Tan, G.; Sun, W.; Xu, Y.; Wang, H.; Xu, N. Sorption of mercury (II) and atrazine by biochar, modified biochars and biochar based activated carbon in aqueous solution. *Bioresour. Technol.* **2016**, *211*, 727−735.

(4) Sun, Q.; Aguila, B.; Perman, J.; Earl, L. D.; Abney, C. W.; Cheng, Y.; Wei, H.; Nguyen, N.; Wojtas, L.; Ma, S. Postsynthetically modified covalent organic frameworks for efficient and effective mercury removal. *J. Am. Chem. Soc.* **2017**, *139*, 2786−2793.

(5) Kończyk, J.; Żarska, S.; Ciesielski, W. Adsorptive removal of Pb (II) ions from aqueous solutions by multi-walled carbon nanotubes functionalised by selenophosphoryl groups: Kinetic, mechanism, and thermodynamic studies. *Colloids Surf., A* **2019**, *575*, 271−282.

(6) Alhumaimess, M. S. Sulfhydryl functionalized activated carbon for Pb (II) ions removal: kinetics, isotherms, and mechanism. *Sep. Sci. Technol.* **2020**, *55*, 1303−1316.

(7) Stando, G.; Hannula, P.-M.; Kumanek, B.; Lundström, M.; Janas, D. Copper recovery from industrial wastewater-Synergistic electrodeposition onto nanocarbon materials. *Water Resour. Ind.* **2021**, *26*, No. 100156.

(8) Das, A.; Bar, N.; Das, S. K. Pb (II) adsorption from aqueous solution by nutshells, green adsorbent: Adsorption studies, regeneration studies, scale-up design, its effect on biological indicator and MLR modeling. *J. Colloid Interface Sci.* **2020**, *580*, 245−255.

(9) Nag, S.; Bar, N.; Das, S. K. Sustainable bioremadiation of Cd (II) in fixed bed column using green adsorbents: Application of Kinetic models and GA-ANN technique. *Environ. Technol. Innovations* **2019**, *13*, 130−145.

(10) Nag, S.; Mondal, A.; Roy, D. N.; Bar, N.; Das, S. K. Sustainable bioremediation of Cd (II) from aqueous solution using natural waste materials: kinetics, equilibrium, thermodynamics, toxicity studies and GA-ANN hybrid modelling. *Environ. Technol. Innovations* **2018**, *11*, 83−104.

(11) Castro-Muñoz, R.; González-Melgoza, L. L.; García-Depraect, O. Ongoing progress on novel nanocomposite membranes for the separation of heavy metals from contaminated water. *Chemosphere* **2021**, *270*, No. 129421.

(12) Hoseinian, F. S.; Rezai, B.; Kowsari, E.; Chinnappan, A.; Ramakrishna, S. Synthesis and characterization of a novel nano-collector for the removal of nickel ions from synthetic wastewater using ion flotation. *Sep. Purif. Technol.* **2020**, *240*, No. 116639.

(13) Nguyen, M. K.; Pham, T. T.; Pham, H. G.; Hoang, B. L.; Nguyen, T. H.; Nguyen, T. H.; Tran, T. H.; Ngo, H. H.; et al. Fenton/ozone-based oxidation and coagulation processes for removing metals (Cu, Ni)-EDTA from plating wastewater. *J. Water Process Eng.* **2021**, *39*, No. 101836.

(14) Ayub, S.; Siddique, A. A.; Khursheed, M. S.; Zarei, A.; Alam, I.; Asgari, E.; Changani, F. Removal of heavy metals (Cr, Cu and Zn) from electroplating wastewater by electrocoagulation and adsorption processes. *Desalin. Water Treat.* **2020**, *179*, 263−271.

(15) Honarmandrad, Z.; Javid, N.; Malakootian, M. Efficiency of ozonation process with calcium peroxide in removing heavy metals (Pb, Cu, Zn, Ni, Cd) from aqueous solutions. *SN Appl. Sci.* **2020**, *2*, No. 703.

(16) Waly, S. M.; El-Wakil, A. M.; Abou El-Maaty, W. M.; Awad, F. S. Efficient removal of Pb (II) and Hg (II) ions from aqueous solution by amine and thiol modified activated carbon. *J. Saudi Chem. Soc.* **2021**, *25*, No. 101296.

(17) Awad, F. S.; Bakry, A. M.; Ibrahim, A. A.; Lin, A.; El-Shall, M. S. Thiol-and Amine-Incorporated UIO-66-NH_2 as an Efficient Adsorbent for the Removal of Mercury (II) and Phosphate Ions from Aqueous Solutions. *Ind. Eng. Chem. Res.* **2021**, *60*, 12675−12688.

(18) Berber, M. R. Surface-functionalization of activated carbon with polyglucosamine polymer for efficient removal of cadmium ions. *Polym. Compos.* **2020**, *41*, 3074−3086.

(19) Sharififard, H.; Rezvanpanah, E.; Rad, S. H.; et al. A novel natural chitosan/activated carbon/iron bio-nanocomposite: Sonochemical synthesis, characterization, and application for cadmium removal in batch and continuous adsorption process. *Bioresour. Technol.* **2018**, *270*, 562−569.

(20) Sharma, G.; Naushad, M. Adsorptive removal of noxious cadmium ions from aqueous medium using activated carbon/zirconium oxide composite: isotherm and kinetic modelling. *J. Mol. Liq.* **2020**, *310*, No. 113025.

(21) Tang, N.; Niu, C.-G.; Li, X.-T.; Liang, C.; Guo, H.; Lin, L.-S.; Zheng, C.-W.; Zeng, G.-M. Efficient removal of Cd^{2+} and Pb^{2+} from aqueous solution with amino-and thiol-functionalized activated carbon: Isotherm and kinetics modeling. *Sci. Total Environ.* **2018**, *635*, 1331−1344.

(22) Wan Ibrahim, W. M. H.; Amini, M. H. M.; Sulaiman, N. S.; Kadir, W. R. W. A. Evaluation of alkaline-based activated carbon from

https://doi.org/10.1021/acsomega.1c06441
ACS Omega 2022, 7, 6058−6069

Leucaena Leucocephala produced at different activation temperatures for cadmium adsorption. *Appl. Water Sci.* **2021**, *11*, 1−13.
(23) Xie, X.; Gao, H.; Luo, X.; Su, T.; Zhang, Y.; Qin, Z. Polyethyleneimine modified activated carbon for adsorption of Cd (II) in aqueous solution. *J. Environ. Chem. Eng.* **2019**, *7*, No. 103183.
(24) Nazerdeylami, S.; Zare-Dorabei, R. Simultaneous adsorption of Hg^{2+}, Cd^{2+} and Cu^{2+} ions from aqueous solution with mesoporous silica/DZ and conditions optimise with experimental design: kinetic and isothermal studies. *Micro−Nano Lett.* **2019**, *14*, 823−827.
(25) Chen, Z.; Tang, B.; Niu, Y.; Chen, H.; Liu, Y.; Wang, A.; Bai, L. Synthesis of silica supported thiosemicarbazide for Cu (II) and Zn (II) adsorption from ethanol: A comparison with aqueous solution. *Fuel* **2021**, *286*, No. 119287.
(26) Wu, J.; Mario, E. D. A.; Yang, B.; Liu, C.; Jia, F.; Song, S. Efficient removal of Hg^{2+} in aqueous solution with fishbone charcoal as adsorbent. *Environ. Sci. Pollut. Res.* **2018**, *25*, 7709−7718.
(27) Huang, N.; Zhai, L.; Xu, H.; Jiang, D. Stable covalent organic frameworks for exceptional mercury removal from aqueous solutions. *J. Am. Chem. Soc.* **2017**, *139*, 2428−2434.
(28) Peng, Y.; Huang, H.; Zhang, Y.; Kang, C.; Chen, S.; Song, L.; Liu, D.; Zhong, C. A versatile MOF-based trap for heavy metal ion capture and dispersion. *Nat. Commun.* **2018**, *9*, No. 187.
(29) Luo, F.; Chen, J. L.; Dang, L. L.; Zhou, W. N.; Lin, H. L.; Li, J. Q.; Liu, S. J.; Luo, M. B. High-performance Hg^{2+} removal from ultra-low-concentration aqueous solution using both acylamide-and hydroxyl-functionalized metal−organic framework. *J. Mater. Chem. A* **2015**, *3*, 9616−9620.
(30) Piri, S.; Zanjani, Z. A.; Piri, F.; Zamani, A.; Yaftian, M.; Davari, M. Potential of polyaniline modified clay nanocomposite as a selective decontamination adsorbent for Pb(II) ions from contaminated waters; kinetics and thermodynamic study. *J. Environ. Health Sci.* **2016**, *14*, No. 20.
(31) Barakat, M. A. New trends in removing heavy metals from industrial wastewater. *Arab. J. Chem.* **2011**, *4*, 361−377.
(32) Mitra, T.; Singha, B.; Bar, N.; Das, S. K. Removal of Pb (II) ions from aqueous solution using water hyacinth root by fixed-bed column and ANN modeling. *J. Hazard. Mater.* **2014**, *273*, 94−103.
(33) Zare-Dorabei, R.; Ferdowsi, S. M.; Barzin, A.; Tadjarodi, A. Highly efficient simultaneous ultrasonic-assisted adsorption of Pb (II), Cd (II), Ni (II) and Cu (II) ions from aqueous solutions by graphene oxide modified with 2, 2′-dipyridylamine: central composite design optimization. *Ultrason. Sonochem.* **2016**, *32*, 265−276.
(34) Keramat, A.; Zare-Dorabei, R. Ultrasound-assisted dispersive magnetic solid phase extraction for preconcentration and determination of trace amount of Hg (II) ions from food samples and aqueous solution by magnetic graphene oxide (Fe_3O_4@ GO/2-PTSC): Central composite design optimization. *Ultrason. Sonochem.* **2017**, *38*, 421−429.
(35) Zhou, Y.; Luan, L.; Tang, B.; Niu, Y.; Qu, R.; Liu, Y.; Xu, W. Fabrication of Schiff base decorated PAMAM dendrimer/magnetic Fe_3O_4 for selective removal of aqueous Hg (II). *Chem. Eng. Sci.* **2020**, *398*, No. 125651.
(36) Luan, L.; Tang, B.; Liu, Y.; Wang, A.; Zhang, B.; Xu, W.; Niu, Y. Selective capture of Hg (II) and Ag (I) from water by sulfur-functionalized polyamidoamine dendrimer/magnetic Fe_3O_4 hybrid materials. *Sep. Purif. Technol.* **2021**, *257*, No. 117902.
(37) Monier, M.; Elsayed Nadia, H.; Abdel-Latif, D. A. Synthesis and application of ion-imprinted resin based on modified melamine−thiourea for selective removal of Hg(II). *Polym. Int.* **2015**, *64*, 1465−1474.
(38) Yuan, X.; Luo, K.; Zhang, K.; He, J.; Zhao, Y.; Yu, D. Combinatorial Vibration-Mode Assignment for FTIR Spectrum of Crystalline Melamine: a Strategic Approach towards Theoretical IR Vibrational Calculations of Triazine-Based Compounds. *J. Phys. Chem. A* **2016**, *120*, 7427−7433.
(39) Zhu, H.; Xu, S.-a. Preparation and fire behavior of rigid polyurethane foams synthesized from modified urea−melamine−formaldehyde resins. *RSC Adv.* **2018**, *8*, 17879−17887.
(40) Ganesan, K.; Ratke, L. Facile preparation of monolithic κ-carrageenan aerogels. *Soft Matter* **2014**, *10*, 3218−3224.
(41) Zhang, S.; Zeng, M.; Xu, W.; Li, J.; Li, J.; Xu, J.; Wang, X. Polyaniline nanorods dotted on graphene oxide nanosheets as a novel super adsorbent for Cr (VI). *Dalton Trans.* **2013**, *42*, 7854−7858.
(42) Liu, Z.; Sun, Y.; Xu, X.; Qu, J.; Qu, B. Adsorption of Hg (II) in an Aqueous Solution by Activated Carbon Prepared from Rice Husk Using KOH Activation. *ACS Omega* **2020**, *5*, 29231−29242.
(43) Bakry, A. M.; Awad, F. S.; Bobb, J. A.; Ibrahim, A. A.; El-Shall, M. S. Melamine-based functionalized graphene oxide and zirconium phosphate for high performance removal of mercury and lead ions from water. *RSC Adv.* **2020**, *10*, 37883−37897.
(44) Awad, F. S.; AbouZied, K. M.; Abou El-Maaty, W. M.; El-Wakil, A. M.; El-Shall, M. S. Effective removal of mercury (II) from aqueous solutions by chemically modified graphene oxide nanosheets. *Arab. J. Chem.* **2020**, *13*, 2659−2670.
(45) Awad, F. S.; AbouZied, K. M.; Bakry, A. M.; Abou El-Maaty, W. M.; El-Wakil, A. M.; El-Shall, M. S. Polyacrylonitrile modified partially reduced graphene oxide composites for the extraction of Hg (II) ions from polluted water. *J. Mater. Sci.* **2021**, *56*, 7982−7999.
(46) Sitko, R.; Musielak, M.; Serda, M.; Talik, E.; Zawisza, B.; Gagor, A.; Malecka, M. Thiosemicarbazide-grafted graphene oxide as superior adsorbent for highly efficient and selective removal of mercury ions from water. *Sep. Purif. Technol.* **2021**, *254*, No. 117606.
(47) Bakry, A. M.; Awad, F. S.; Bobb, J. A.; El-Shall, M. S. Multifunctional Binding Sites on Nitrogen-Doped Carboxylated Porous Carbon for Highly Efficient Adsorption of Pb (II), Hg (II), and Cr (VI) Ions. *ACS Omega* **2020**, *5*, 33090−33100.
(48) Villalobos, M.; Bargar, J.; Sposito, G. Mechanisms of Pb(II) Sorption on a Biogenic Manganese Oxide. *Environ. Sci. Technol.* **2005**, *39*, 569−576.
(49) Naushad, M.; Alqadami, A. A.; Ahamad, T. Removal of Cd (II) ion from aqueous environment using triaminotriethoxysilane grafted oxidized activated carbon synthesized via activation and subsequent silanization. *Environ. Technol. Innovations* **2020**, *18*, No. 100686.
(50) Gatabi, M. P.; Moghaddam, H. M.; Ghorbani, M. Efficient removal of cadmium using magnetic multiwalled carbon nanotube nanoadsorbents: equilibrium, kinetic, and thermodynamic study. *J. Nanopart. Res.* **2016**, *18*, No. 189.
(51) Fu, L.; Wang, S.; Lin, G.; Zhang, L.; Liu, Q.; Fang, J.; Wei, C.; Liu, G. Post-functionalization of UiO-66-NH2 by 2,5-Dimercapto-1,3,4-thiadiazole for the high efficient removal of Hg(II) in water. *J. Hazard. Mater.* **2019**, *368*, 42−51.
(52) Geisse, A.; Mutuku, N.; Genna, D. Removal of Lead Ions from Water Using Thiophene-functionalized Metal-organic Frameworks. *Chem. Commun.* **2019**, *56*, 237−240.
(53) Li, Z.; Pan, Z.; Wang, Y. Preparation of ternary amino-functionalized magnetic nano-sized illite-smectite clay for adsorption of Pb (II) ions in aqueous solution. *Environ. Sci. Pollut. Res.* **2020**, *27*, 11683−11696.
(54) Soliman, A. M.; Elwy, H. M.; Thiemann, T.; Majedi, Y.; Labata, F. T.; Al-Rawashdeh, N. A. Removal of Pb (II) ions from aqueous solutions by sulphuric acid-treated palm tree leaves. *J. Taiwan Inst. Chem. Eng.* **2016**, *58*, 264−273.
(55) Bouhamed, F.; Elouear, Z.; Bouzid, J.; Ouddane, B. Batch sorption of Pb (II) ions from aqueous solutions using activated carbon prepared from date stones: equilibrium, kinetic, and thermodynamic studies. *Desalin. Water Treat.* **2014**, *52*, 2261−2271.
(56) Bakry, A. M.; Awad, F. S.; Bobb, J. A.; El-Shall, M. S. Multifunctional Binding Sites on Nitrogen-Doped Carboxylated Porous Carbon for Highly Efficient Adsorption of Pb (II), Hg (II), and Cr (VI) Ions. *ACS Omega* **2020**, *5*, 33090−33100.
(57) Sajjadi, S.-A.; Meknati, A.; Lima, E. C.; Dotto, G. L.; Mendoza-Castillo, D. I.; Anastopoulos, I.; Alakhras, F.; Unuabonah, E. I.; Singh, P.; Hosseini-Bandegharaei, A. A novel route for preparation of chemically activated carbon from pistachio wood for highly efficient Pb (II) sorption. *J. Environ. Manage.* **2019**, *236*, 34−44.
(58) Kongsune, P.; Rattanapan, S.; Chanajaree, R. The removal of Pb^{2+} from aqueous solution using mangosteen peel activated carbon:

https://doi.org/10.1021/acsomega.1c06441
ACS Omega 2022, 7, 6058−6069

Isotherm, kinetic, thermodynamic and binding energy calculation. *Groundwater Sustainability Dev.* **2021**, *12*, No. 100524.
(59) Zhao, H.; Song, F.; Su, F.; Shen, Y.; Li, P. Removal of cadmium from contaminated groundwater using a novel silicon/aluminum nanomaterial: an experimental study. *Arch. Environ. Contam. Toxicol.* **2021**, *80*, 234−247.
(60) Li, Y.; Zhou, M.; Waterhouse, G. I.; Sun, J.; Shi, W.; Ai, S. Efficient removal of cadmium ions from water by adsorption on a magnetic carbon aerogel. *Environ. Sci. Pollut. Res.* **2021**, *28*, 5149−5157.

https://doi.org/10.1021/acsomega.1c06441
ACS Omega 2022, 7, 6058−6069